A Fast and Practical Imaging Scheme for a Rotating RF Coil at 9.4T by Using Ultra-short TE Sequence in Radial Trajectory

Mingyan Li[1], Thimo Hugger[2], Ewald Weber[1], Jin Jin[1], Feng Liu[1], Peter Ullmann[2], Simon Stark[2], Yasvir Tesiram[3], Yang Yang[1], Sven Junge[2], and Stuart Crozier[1]

[1]*The School of Information Technology and Electrical Engineering, The University of Queensland, Brisbane, QLD, Australia,* [2]*Bruker BioSpin MRI GmbH, Ettlingen, Baden-Württemberg, Germany,* [3]*Centre for Advanced Imaging, The University of Queensland, Brisbane, QLD, Australia*

Target audience: Researchers who are interested in novel RF coil, non-Cartesian sampling and alternative imaging techniques at ultra-high fields.

Purpose: The rotating RF coil (RRFC) [1] and rotating RF coil array (RRFCA) [2] employ rotation-associated spatial varying sensitivity to reconstruct images with reduced scan duration. However, acquiring and calibrating sensitivity map is not a trivial task, especially at ultra high fields. Without considering the varying sensitivity, the direct application of inverse fast Fourier transform (IFFT) to the *k*-space data sampled in Cartesian trajectory yields fold-over artefacts, similar to those in parallel imaging [3]. In this work, we propose an alternative, practical imaging scheme by using the ultra-short TE (UTE) sequence with radial trajectory [4] for a single channel RRFC without sensitivity mapping. Simulations and experimental data are used to analyse and validate the feasibility of this imaging method.

Methods: One of the most prominent features of radial trajectory is the oversampling of the central *k*-space, where the redundant acquisition provides averaging effect that improves the robustness against subject motion [5, 6]. Fig.1(a) illustrates the number of acquisitions for the points on a radial line passing the centre of *k*-space. The centre point is sampled 804 times with 804 centre-to-out spokes; while other points in the central region are sampled at least 20 times. The final value of each *k*-space data b_k at location *k*, is calculated in Eq.1 as an average of a series of samplings $b_{k,\alpha}$. Each of these samples corresponds to sensitivity at various angular positions (from α_1 to α_s) of the coil. The *k*-space data generation is illustrated in Eq.2 in a matrix form. The proton density ρ is encoded with the encoding matrix *E*, which is the dot product of the standard Fourier weighting $e_{k,r}$ and sensitivity weighting $S_{\alpha,r}$, where *k, r and* α are indices for *k*-space coordinates, voxel coordinates and angular positions, respectively. Their ranges are $[1,N^2]$, provided the image resolution is $N\times N$. In the transceive mode, *S* denotes the composite sensitivity that accounts for both the transmit and receive profiles. For a stationary coil, the sensitivity weightings of each row in the matrix *E* are identical ($\alpha_1 = \alpha_2 = \dots \alpha_n$). Therefore, the sensitivity weightings in matrix *E* can be extracted out and form a diagonal matrix *diag(S)*. The image can be obtained by applying IFFT (F^{-1}) to the *k*-space data as: $m=F^{-1}Fdiag(S)\rho=diag(S)\rho$. In contrast, for the data sampled with a rotating coil in Cartesian trajectory, the sensitivity weightings in each row are different and *S* cannot be separated from the matrix *E* anymore. Consequently, the operation $F^{-1}(F\cdot S)\rho$ yields an image with fold-over artefacts. In a radial trajectory, however, the equivalent sensitivity weighting $\overline{S_k}$ at location *k*, is an average of the sensitivity maps of all the visited angular positions, as illustrated in Eq.1. The magnitude and phase of the averaged sensitivity are illustrated in Fig.1(b). The uniformity of the equivalent sensitivity $\overline{S_k}$ can be dramatically improved with as few as three samples with an appropriate angular increment θ (the position difference of the coil when two adjacent spokes are acquired). With six samples, the uniformity of the sensitivity is further improved. This allows the direct application of an inverse Fourier transform to yield artefact-free images. To maximise the uniformity of the equivalent sensitivity $\overline{S_k}$, the rotating speed and repetition time (TR) should be adjusted accordingly, so that the repeated samples are acquired at the angular positions uniformly distributed around the subject. In practice, the rotating speed was monitored with an optical sensor built into the RRFC system. Experiments were performed using a single channel RRFC in transceive mode on the 9.4T Bruker Biospin MRI scanner (Ettlingen, Germany). The length (longitudinal) of the rotating coil was 30 mm and the diameter was 40 mm with a 60˚ open angle. The RRFC was pneumatically driven and the mechanical structures were elaborated in a previous publication [1]. A LEGO phantom and a homogeneous phantom were used in the experiment. The radial ultra short TE (radial-UTE) sequence (TE/TR = 0.3481ms/30ms) and the Fast Low Angle SHot (FLASH) sequence (TE/TR = 4ms/30ms) were used with radial and Cartesian trajectories, respectively. Data collected using both trajectories were reconstructed by the algorithms available with the scanner software (Paravision). The radial-UTE used half-length spokes, from the centre to the outer k-space.

$$b_k = \frac{1}{s}\left(\sum_{\alpha=\alpha_1}^{\alpha_s} b_{k,\alpha}\right) = \frac{1}{s}\left(\sum_{\alpha=\alpha_1}^{\alpha_s}\sum_{r=1}^{n} e_{k,r}\cdot S_{\alpha,r}\cdot\rho_r\right)$$

$$= \sum_{r=1}^{n} e_{k,r}\cdot\frac{1}{s}\left(\sum_{\alpha=\alpha_1}^{\alpha_s} S_{\alpha,r}\right)\cdot\rho_r = \sum_{r=1}^{n} e_{k,r}\cdot\overline{S_k}\cdot\rho_r \qquad (1)$$

$$\begin{bmatrix} b_1 \\ b_2 \\ \vdots \\ b_k \\ \vdots \\ b_n \end{bmatrix}_{k} = \underbrace{\begin{bmatrix} e_{1,1}S_{\alpha_1,1} & e_{1,2}S_{\alpha_1,2} & \cdots & e_{1,r}S_{\alpha_1,r} & \cdots & e_{1,n}S_{\alpha_1,n} \\ e_{2,1}S_{\alpha_2,1} & e_{2,2}S_{\alpha_2,2} & \cdots & e_{2,r}S_{\alpha_2,r} & \cdots & e_{2,n}S_{\alpha_2,n} \\ \vdots & \vdots & \ddots & \vdots & \vdots & \vdots \\ e_{k,1}S_{\alpha_1,1} & e_{k,2}S_{\alpha_1,2} & \cdots & e_{k,r}S_{\alpha_1,r} & \cdots & e_{k,n}S_{\alpha_1,n} \\ \vdots & \vdots & \cdots & \vdots & \ddots & \vdots \\ e_{n,1}S_{\alpha_n,1} & e_{n,2}S_{\alpha_n,2} & \cdots & e_{n,r}S_{\alpha_n,r} & \cdots & e_{n,n}S_{\alpha_n,n} \end{bmatrix}}_{\text{Encoding matrix } E=F\cdot S} \underbrace{\begin{bmatrix} \rho_1 \\ \rho_2 \\ \vdots \\ \rho_r \\ \vdots \\ \rho_n \end{bmatrix}}_{\text{proton density}} \qquad (2)$$

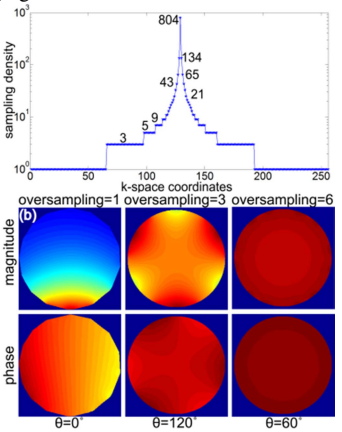

Fig.1 (a) Sampling density. (b) Averaged sensitivity with various oversamplings.

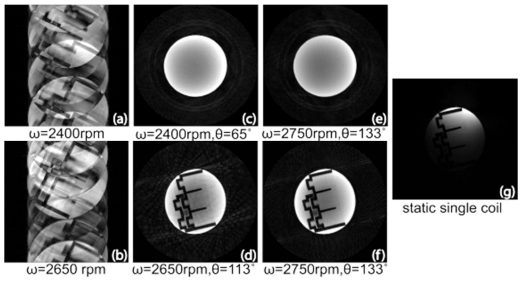

Fig. 2 (a) and (b), reconstructions from Cartesian sampling at 2400 rpm and 2650 rpm. (c) and (d), reconstructions from radial sampling at the same speed as (a) and (b), respectively. (e) and (f), repeating (c) and (d) at 2750 rpm. (g) Image acquired with the RRFC but as a static coil.

Results: The reconstructed images are shown in Fig. 2. The pre-set rotating speed (rpm) and the average of the measured angular increment are listed below the images. Fig. 2 (a) and (b) are images reconstructed from Cartesian *k*-space data that exhibit strong ghost artefacts. At the same rotating speeds, the standard regridding/IFFT algorithm produces good reconstructions regardless of the changing sensitivity, for both the homogeneous and LEGO phantoms as shown in Fig. 2(c) and (d), respectively. Various rotating speeds were tested while TR was kept constant. The best image reconstruction was found at speed of 2750 rpm as shown in Fig. 2(e) and (f). The RRFC was also used as a static coil to acquire an image for the LEGO phantom as shown in Fig. 2(g). Fig. 2 clearly demonstrates that by combining the radial sampling with the rotating technique, the single element RRFC is capable of producing good quality uniform images by standard algorithm, without mapping the rotation-dependent sensitivity maps.

Discussion: The air flow to drive the turbines experienced minor fluctuations and generated a small variation in speed ($\leq 5\%$) and angular increment. These variations did not affect the image quality. We found that the angular increment θ was critical to the quality of the image reconstruction. Good image reconstructions were found with the angular increments of 133º/113º, 93º, 65º, which approximately correspond to 3, 4 and 6 repeated samplings to generate a uniform sensitivity. This correlates well with the simulation results shown in Fig. 1(b).

Conclusion: In this proof of concept study at 9.4T, the averaging effect of radial sampling for RRFC was investigated and the rotation-related motion artefacts were suppressed with optimal rotating speed. The results indicate that using radial trajectory, the single element RRFC is capable of reconstructing good quality images without using sensitivity calibration. It is hoped that this novel imaging method will facilitate human imaging at ultra high fields, especially multi-nuclear imaging, while RF elements for several x-nuclei can be accommodated in the same rotating structure. Future work includes designing RF elements for simultaneous x-nuclei imaging and exploring the undersampling of radial acquisition with RRFCA for real-time imaging.

References: 1. Trakic A, et al, *JMR*, 2009, 201. 2:186-198. 2. Li M, et al , *JMR,* 2014, 240: 102-12. 3. Pruessman KP, et al, *MRM*, 1999 Nov; 42 (5): 952-62.4. Lauterbur PC, *Nature*, 1973, 242:190–191.5 Trouard TP, et al, *JMRI* 1996, 6(6): 925-35. 6. Katoh M, et al, *JMRI* 2006, 23(5): 757-62

Acknowledgement: This research was supported under Australian Research Council's *Linkage Projects* scheme with Bruker Biospin (Germany).